Studies of internal stress induced by solidification of menthol melt as temporary consolidant in archaeological excavations using resistance strain gauge method

Xiuxiu Chen
Shanghai University
Yang Xu
Shanghai University
Ming Chen
Shanghai University
Xiao Huang (xhuang@shu.edu.cn)
Shanghai University https://orcid.org/0000-0002-9028-5964
Hongjie Luo
Shanghai University
Yicheng Song
Shanghai University

Research article

Keywords: Menthol, Temporary consolidation, Archaeological excavation, Internal stress

Posted Date: June 4th, 2020

DOI: https://doi.org/10.21203/rs.3.rs-17945/v2

Version of Record: A version of this preprint was published on July 9th, 2020. See the published version at https://doi.org/10.1186/s40494-020-00414-y.

Abstract

Volatile organic solids, such as cyclododecane or menthol, have been employed as temporary reinforcement material during archaeological excavations. They are usually applied as melts and reinforcement is achieved once the melts solidify. Such solidification process can induce internal stress on the artifacts, which can be a big concern, especially to those very precious and fragile ones. However, information about such stress is still extremely limited at present. This paper proposes an experimental method based on resistance strain gauge technique to monitor the deformation induced by solidification of menthol melt. Bending tests are performed on very thin glass slides. The solidification process of menthol melt is well characterized by the development of mechanical strains. Then, menthol melts are applied to three kinds of simulated samples, i.e. glass, sandstone and rice paper, to investigate the mechanical response of preserved bodies upon solidification. It is found that menthol melt will generate certain amount expansion or contraction of the objects upon solidification. The stresses induced, evaluated according to obtained strains, are generally quite small, indicating that application of menthol as reinforcement material is safe in mechanics for cultural relics.

1. Introduction

At archaeological excavation sites, on-site consolidation is an important and widely applied conservation technique. Inorganic materials such as plaster[1-5] as well as organic synthetic polymers such as polyurethanes[6-9], polyacrylates[10-11] and epoxy resins[12-13] are all used to consolidate cultural relics on-site. However, application of these materials are subjected to an obvious drawback that they are very difficult, sometimes even impossible, to be removed afterwards. This would bring some negative effects on following archaeological research and conservation work.

Recently, on-site temporary consolidation has attracted more and more attention due to its reversibility. Cyclododecane (CDD)[14-21] and menthol[22-25], also referred as “volatile binder media”[23-24], are mostly used temporary consolidants. In typical applications, the material is melted and applied on the target cultural relics. And then, the consolidated relics can be transported safely to museums or laboratories, where the consolidants can be completely removed easily via sublimation. Residue free is the most popular character of this temporary consolidation technique, since there is no consolidation molecules left to interfere with future archaeological research and conservation work. Detailed application procedures are provided elsewhere in literature[16, 21, 23].

Internal stress can be induced by solidification of an organic melt due to factors such as volumetric shrinkage, thermal stress etc[26,27]. Internal stress is one of the most common reasons for material failures[27]. Thus, it arouses our attention and interest in investigating possible internal stress induced on the artifacts during temporary consolidation practice. Although successful applications of CDD and menthol as consolidant have demonstrated their safety to cultural heritages[14-25], vital information about the internal stress such as generation mechanism, magnitude and distribution, which can be interesting and helpful to conservators, is still unclear.

Internal stress is very difficult to observe, recognize and measure directly. Many indirect methods have been invented and developed to measure internal stress of different types and forms of materials[28-35]. Among these methods, resistance strain gauge[33-35] is a commonly used strain measurement device. Its working principle is that the electrical resistance of its metal part changes linearly with its deformation[36]. Resistance strain gauge method has been widely used in measuring the internal stress of railways[37], bridges[38], building constructions[39], reinforced concrete components[40] etc. Plenty of applications have shown that resistance strain gauge measurement is a fast, sensitive, accurate and reliable method. Meanwhile, the measurement does not change the original stress state of test objects.

In this paper, resistance strain gauge measurement method is introduced into the study of internal stress induced by solidification of menthol melts. Three different simulated samples, i.e. sandstone, glass and rice paper, are chosen to simulate the materials usually found in archaeological excavations. Information of such internal stresses about its generation mechanism, distribution and magnitude is revealed for the first time.

2. Experimental

2.1 Materials

L-menthol (99%, melting point 43°C; see Figure 1) is purchased from Aldrich Co., used as received. The substrates used for internal stress experiments are commercial glass (glass I: 18mm×18mm×0.12mm; glass II: 25mm×75mm×1mm), sandstone from Yungang Grottos (size: 25mm×75mm×2mm) and commercial rice paper (size: 25mm×75mm×0.01mm). The Yungang sandstone used has a porosity of 6.93% and median pore size of 505nm based on MIP measurement.

2.2 Instrumentation

The elastic moduli of rice paper and sandstone were measured by an electronic universal testing machine (BZ2.5/TS1S Zwick/Roell, Germany). The elastic modulus of glass was measured by a solid material dynamic elastic property tester (China Building Materials Test and Certification Group Co., Ltd. DST-III).

The strain was measured by a DH3818Y static stress tester (Jiangsu Donghua Testing Technology Co., China). The strain gauges used were model BE120-3AA (Jiangsu Donghua Testing Technology Co., China) with temperature self-compensation function, resistance of 120.1±0.2 Ω and gauge factor of 2.00-2.20.

As shown in Figure 2, the strain gauge has layered structure, in which a sensitive grid made of thin metal foil (2.8mm×2.0mm) is sandwiched between a so-called plastic film (6.4mm×3.5mm) and a laminated film. Because the resistance of the grid is extremely sensitive to strain changes, very small strain changes, as low as to the order of 10^{-6}, can be detected. Equation 1 describes the relation between strain changes and resistance changes of the metal coil. Based on Eq. 1, the changes in resistance can be converted to the strain changes.

$(\Delta R) / R = K \times \varepsilon$ eq.1

Where R strain gauge original resistance in Ω (ohm)

ΔR resistance change caused by elongation or compression in Ω (ohm)

K gauge factor (2.00-2.20)

ε strain

2.3 Experiment setup

In this work, a static resistance stress-strain test setup is applied. As static resistance stress-strain test is very sensitive, the experiments are carried out in a separated room and precautions are taken to avoid possible outside disturbances. A quarter bridge circuit is employed for the testing. The strain gauge is self-compensated with temperature, which can reduce the influence of temperature on the resistance of the variable pieces[41]. In order to prevent interference from other electrical appliances on site, shielded wires are used as connecting wires, and the lengths of all wires are kept the same as 30 cm long to reduce the influence of wire resistance. The strain gauges are carefully sealed to be waterproof and moisture-proof.

The whole gauge is firmly glued (ethyl α-cyanoacrylates glue) on the testing substrate to ensure that the deformation of substrate can be precisely measured by the sensitive grid. Detailed setup is described below. Each strain gauge experiment is performed at least three times to guarantee the reproducibility. A fresh sample is used each time.

2.3.1 Model sample

Two strain gauges were glued to the top and bottom of a glass I sample. Because the electric resistance of strain gauge is affected by temperature, very thin glass substrate (0.12mm in thickness) was used to minimize the strain difference due to temperature gradient across glass thickness. Vertical plastic tape was wrapped around to build a sink to accommodate the melted menthol, as demonstrated in Figure 3. Then, 0.1, 0.5, 1, and 2mL of menthol melts of 60 or 80°C were cast on the samples respectively. Strains were measured and recorded on site during the whole solidification process.

2.3.2 Simulated samples

The strains were measured for three different simulated materials. In each experiment, two strain gauges were glued at two positions. One position is where menthol melt is applied, and the other position is away from applying position.

3. Results And Discussions

3.1 Static resistance stress-strain tests on model samples

Figure 4 provides the variation of strains and temperature with respect to operation time. It appears that the strain gauge on the top of glass I sample (where melted menthol is applied) provides negative values indicating compression. Meanwhile, the other strain gauge on the bottom of glass provides positive values which suggest tensile deformation. It is known that solidification of menthol melt is accompanied by volumetric shrinkage[24], which leads to concave bending of the glass I sample in the present experiment. This bending results in compression and stretching, respectively, in the upper and lower portion of glass, in consistent with the measurements of strain gauges. Figure 4 also shows that the two strain curves provided by upper and bottom strain gauges are roughly symmetrical about the horizontal axis which indicates zero strain.

Combined with temperature curve, more information can be read from Figure 4. When menthol melt is just applied, i.e. before 500 seconds, low level strain noises were observed due to thermal impacts. After that, from 500 seconds to 1000 seconds is an early stage of solidification. In this stage, temperature decreases below the melting point of menthol and both compressive and tensile strains start to increase, indicating that the volumetric shrinkage of menthol upon solidification starts to lead to bending of glass substrate. From 1000 seconds to about 2000 seconds is the steady stage of solidification. In this stage, temperature rises again due to exothermic solidification process. When the thermal balance is established between internal heat generation and diffusion to outside ambience, the temperature becomes stable, indicating a stable solidification stage. In this stage, the strains increase with nearly constant gradients, implying that menthol solidifies in a constant rate. Completion of solidification is found around 2000 seconds, from when the temperature drops again due to termination of exothermic solidification. At the same time, both strains reach peak values and then stop increasing. This verifies the completion of solidification from mechanical view, i.e. menthol stops to shrinkage and, therefore, is unable to cause further bending of glass. The period after 2000 seconds is a relaxation stage. In this stage, temperature gradually lowers down showing that no solidification reaction takes place. The strains decrease slightly, probably due to structural relaxation/rearrangement which is often observed in imperfectly crystallized polymers[42].

Figure 4 provides an important insight to the application of menthol for temporary conservation. In real applications, although white waxy solid can be observed just a few minutes after menthol melt is applied, it is still difficult for people to tell whether solidification is completed. Our experiment shows that the solidification of menthol takes much long time than we expected and the solidification achieves peak mechanical strength in about 2000 seconds. When melted menthol is applied in archaeological excavations, enough time should be given to enable the menthol solidifies completely for a higher strength.

Figures 5a and 5b are prepared to discuss the impacts of menthol quantities and melt temperatures on solidification, respectively. Figure 5a shows that application of more menthol leads to longer solidification time as well as higher strains. This indicates that stronger stress effects would be induced in applications of large quantities of menthol. Figure 5b illustrates that application of menthol melts of higher temperature would enhance the bending deformation of glass substrate and lead to larger strains.

3.2 Static resistance stress-strain tests on simulated samples

Previous studies have characterized the solidification process of menthol using a model sample. In this part we will focus on samples closer to real cases in conservation of cultural relics. Three simulated samples are investigated, i.e. glass II, Yungang sandstone and rice paper, representing rigid non-porous, rigid porous and soft materials, respectively. These are all common materials encountered during excavations. The resistance strain gauges need to be glued on the samples firmly. Thus, for the convenience and practicality of the research work, non-aged simulated samples with relative strong mechanical strength are used. Based on the basic physical understanding of this phenomenon, the occurrence of inner stress should not be related to whether samples are aged or fragile. The outcomes of inner stress are closely related to the status of the samples. So, the results obtained should be applicable to aged or fragile artifacts as found in archaeological excavations.

As demonstrated in Figures 6-8, two strain gauges are pasted on one side of each sample. In order to investigate the comprehensive stress profile induced due to menthol application, one gauge denoted by “O” is in the region where menthol melt is applied, the other one denoted by “A” is away from melt application. Precautions have been taken to prevent outflow of menthol melt.

The results on rigid non-porous glass II samples are shown in Figure 6. The stain curves are divided into 2 regions. The first region, from 0 to about 400 second, is an invalid phase as the signals are mainly induced by thermal impact of high temperature melts. After 400 seconds, increasing strain at position O is observed, indicating solidification of menthol melt. The negative values indicate compression, in consistent with model sample (glass I). The strain reaches maximum value at around 1000 seconds, much faster than it does in glass I sample. This is because in glass II case, the melt is cooled down much faster. After 1000 seconds, the strain starts to gradually decrease due to some degree of structural rearrangement before it stabilizes[42]. For position A, strain just oscillates in a small range around zero strain except the first invalid stage. It indicates that the stress in the region outside menthol application is basically unaffected by the solidification of menthol.

Yungang sandstone, representative of rigid porous material, is also investigated. In Figure 7a, when menthol melt is applied on position O, strain at the O changes rapidly due to thermal impact. After that, when the melt starts to solidify, strain at position O switches quickly from negative to positive side, indicating that solidification of menthol melt finally leads to facial stretching of sandstone. This phenomenon may be attributed to the porous microstructure of sandstone. When applied, melted menthol might permeate into the porous sandstone. It is speculated that solidification of menthol inside the micro pores would generates expansion actions on the pore walls, resulting in stretching of sample. The strain of position A is around -10, indicating weak compressive stress. This is reasonable as the stretching of the small core area has to be balanced by the compression of surrounding area.

In order to verify the proposed mechanism above, two more sets of experiments are carried out on sandstones. As shown in Figure 6b, four strain gauges, referred as 1 (top), 2 (top), 3 (bottom), and 4

(bottom), are glued on both sides of the sandstone. 2mL of menthol melt is applied. It can be seen from the figure that both gauge 1 and 2 provide positive values indicating tensile strain in the upper portion, while gauge 3 and 4 show negative values indicating compressive deformation in the lower portion.

In another test shown in Figure 7c, much less menthol melt is applied. In this case, variation of strain is a bit similar to that applied on glass. The strain at position O is always negative. This suggests that the little menthol mainly solidifies on the surface of sandstone instead of infiltrating into the pores due to fast cooling. The surface deformation is therefore contraction.

Rice paper, representative of soft material, is also tested, as seen in Figure 8. As paper does not conduct heat well, thermal influence on the strain at position A is insignificant. It is seen that the strain at position O stabilizes at, which is larger than that of glass II and sandstone. This is because paper is too soft to withstand the contraction of menthol. Unlike rigid samples, the strain at position A of rice paper is also compressive, the same as position O. It suggests that the contraction of the menthol area may lead to contraction in larger neighboring area in soft substrate.

3.3 Stress evaluations of solidification of menthol melts on simulated samples

The information revealed by the static resistance stress-strain tests is the strain of certain media upon solidification of menthol melt. It is quite straight forward according to elastic constitutive that stress strain relation is:

$$\sigma \text{ (stress)} = E \text{ (Elastic Modulus)} \times \varepsilon \text{(strain)} \qquad eq.2$$

The elastic modulus of glass II sample is acquired to be 71.52 GPa by dynamic elastic modulus measurement method. The elastic moduli of Yungang sandstone and rice paper are 3.08 and 1.12 GPa, which are acquired by compression or tensile method on a universal mechanical testing machine respectively. The maximum strain values of point O (position where menthol melt is applied) in each figure are chosen to calculate the stress. The internal stress induced by menthol melts on glass (Figure 6), sandstone (Figure 7a) and rice paper (Figure 8) is calculated to be 0.71, 0.11 and 0.39 MPa, respectively. Although these data might not be very accurate, the order of the magnitudes is acceptable. It shows that all the stresses are quite small. Application of menthol as temporary conservation material is safe to cultural heritages from mechanical viewpoint.

4. Conclusion

On-site temporary consolidation becomes more and more popular during archaeological excavations. Consolidation is achieved after consolidant melts solidify. Internal stress can be induced during solidification which arouses concerns of safety to heritages from material scientists and conservators.

In this work, the internal stress generated by the solidification of menthol melt, is studied by resistance strain gauge method. The results show that small organic molecules, like menthol, will generate certain amount of stress on the objects upon solidification due to volumetric shrinkage. The magnitudes of the

strain and stress are affected by the amount and the temperature of melt applied. For very delicate relics, less and cooler melts should be considered in order to reduce stress.

Detailed studies on three different substrates further show that the nature of the stress is not always compression. For porous objects, which are very commonly observed on an excavation sites, tensile stress may also occur. Meanwhile, the stress can be transmitted to neighboring areas other than the area where the melt is applied, especially in flexible objects. Thus, special attention should be given to relics like paper, fabrics etc.

Overall, such internal stress is generally quite small. On-site temporary consolidation using melted menthol is quite safe to fragile cultural heritages. For the past a few years, nearly 2000 pieces have been consolidated and extracted during excavations using menthol in China.

Abbreviations

CDD: cyclododecane

Declarations

Acknowledgements

The authors are grateful to the financial supports from the National Key Research and Development Program of China (No. 2019YFC1520104, 2019YFC1520504), Key Program of National Natural Science Foundation of China (No. 51732008), Natural Science Foundation of China (No. 11672170) and Shanghai University.

Authors' contributions

XC: conducted most of the experiments and data analyses, wrote the initial draft of this manuscript; YX: implemented the strain gauge experiments and data analyses; MC: implemented the strain gauge experiments; XH: conceptualized the research, interpreted data and finalized the manuscript; HL: helped to design the experiment setup, revised the manuscript; YS: improved the experiment setup, interpreted the data and revised the manuscript. All authors read and approved the final manuscript.

Funding

The research is funded by National Key Research and Development Program of China, Key Program of National Natural Science Foundation of China, Natural Science Foundation of China and Shanghai University.

Availability of data and materials

All data analyzed during this study are included in this published article. Raw data are available upon request.

Competing interest

The authors declare that they have no known competing financial interests or personal relationships that could have appeared to influence the work reported in this paper.

References

1. Ashour T, Wieland H, Georg H, Bockisch FJ, Wu W. The influence of natural reinforcement fibres on insulation values of earth plaster for straw bale buildings. Materials & Design, 2010,31(10), 4676-4685.
2. Bohler J. Simple and inexpensive reinforcement of plaster casts. Der Chirurg, Zeitschrift fur alle Gebiete der operativen Medizen, 1955,26(3), 144.
3. Khenfer MM, Morlier PP. Cellulose fibres reinforced plaster. Materials and Structures, 1999, 32(215), 52-58.
4. Altin S, Anil O, Kopraman Y, Belgin C. Strengthening masonry infill walls with reinforced plaster. Proceedings of the Institution of Civil Engineers-Structures and Buildings, 2010, 163(5), 331-342.
5. Quagliarini E, D'Orazio M. Light Vaults With Frescoes or Stuccoes Strengthened by Glass Fiber-Reinforced Polymer (GFRP) the Role of the Reinforcement on Intrados Strains: First Experimental Data. International Journal of Architectural Heritage, 2010,4(4), 320-336.
6. Li N, Zhao Q, Zhang J, Fu Y, Liu M. A new type of polyurethane polyurea reinforcement material for coal mine. Modern Chemical Industry, 2016,36(10), 126-128.
7. Feng Z. Application of Polyurethane Grouting Material Modified by Silicate to the Reinforcement of Coal Mines Roadway. Journal of Yangtze River Scientific Research Institute, 2013,30(10), 99-103.
8. Linghua TAN, Zhangzhong W, Yuming DAI. Zhixin BA. Progress in Study on the Reinforced Rigid Polyurethane Foams. Materials Review, 2006,20(9), 21-25.
9. Shao-bin Y, Yang Z, Fang-fang C. Development of research on polyurethane grouting materials in mining engineering. Applied Chemical Industry, 2010,39(1), 111-115.
10. Su BM, Zhang HB, Zhang BJ, Jiang DQ, Zhang R, Tan X. A scientific investigation of five polymeric materials used in the conservation of murals in Dunhuang Mogao Grottoes. Journal of Cultural Heritage, 2018,31, 105-111.
11. Cocca M, D'Arienzo L, D'Orazio L, Gentile G, Mancarella C, Martuscelli E, Polcaro C. Water dispersed polymers for textile conservation: a molecular, thermal, structural, mechanical and optical characterisation. Journal of Cultural Heritage, 2006,7(4), 236-243.
12. Briffa SM, Vella DA. The behaviour of as-applied and artificially weathered silica-epoxy consolidants on a typical Mediterranean porous limestone: a comparison with TEOS. Heritage Science, 2019, 30(7), 1-13.

13. Formia A, Tulliani JM, Antonaci P, Sangermano M. Epoxy monomers consolidant for lime plaster cured via a redox activated cationic polymerization. Journal of Cultural Heritage, 2014,15(6), 595-601.
14. Brown M, Davidson A. The Use of Cyclododecane to Protect Delicate Fossils during Transportation. Journal of Vertebrate Paleontology, 2010, 30(1), 300-303.
15. Papini G, Borgioli L, De Luca D, Gui MO, Modugno F. Evaluation of the Effects of Cyclododecane on Oil Paintings. International Journal of Conservation Science, 2018,9(1), 105-116.
16. Stein R, Kimmel J, Marincola M, Klemm F. Observations on cyclododecane as a temporary consolidant for stone. Journal of the American Institute for Conservation, 2000,39(3), 355-369.
17. Bruckle I, Thornton J, Nichols K, Strickler G. Cyclododecane: Technical note on some uses in paper and objects conservation. Journal of the American Institute for Conservation, 1999,38(2), 162-175.
18. Munoz-Vinas S, Vivancos-Ramon V, Ruiz-Segura P. The Influence of Temperature on the Application of Cyclododecane in Paper Conservation. Restaurator-International Journal for the Preservation of Library and Archival Material, 2016,37(1), 29-48.
19. Diaz-Marin C, Aura-Castro E, Sanchez-Belenguer C, Vendrell-Vidal E. Cyclododecane as opacifier for digitalization of archaeological glass. Journal of Cultural Heritage, 2016,17, 131-140.
20. Maish JP, Risser E. A case study in the sue of cyclododecane and latex rubber in the molding of marble. Journal of the American Institute for Conservation, 2002,41(2), 127-137.
21. Vernez D, Wognin B, Tomicic C, Plateel G, Charriere N, Bruhin S. Cyclododecane exposure in the field of conservation and restoration of art objects. International Archives of Occupational and Environmental Health, 2011,84(4), 371-374.
22. Yu Y, Zhang W, Han X, Huang X, Zhao J, Ren Q, Luo H. Menthol-based eutectic mixtures: Novel potential temporary consolidants for archaeological excavation applications. Journal of Cultural Heritage, 2019,39, 103-109.
23. Han X, Rong B, Huang X, Zhou T, Luo H, Wang C. The Use of Menthol as Temporary Consolidant in the Excavation of Qin Shihuang's Terracotta Army. Archaeometry, 2014,56(6), 1041-1053.
24. Han X, Huang X, Zhang BJ. Laboratory Research into the Use of Menthol as a Temporary Consolidant for Conservation on Archaeological Excavations. Archaeometry, 2018,60(6), 1334-1345.
25. Sadek H, Berri BH, Weiss RG. Sublimable layers for protection of painted pottery during desalination. A comparative study. Journal of the American Institute for Conservation, 2018,57(4), 189-202.
26. Roos YH, Karel M, Labuza TP. Melting and Crystallization of Sugars in High-Solids Systems. Journal of Agricultural & Food Chemistry, 2013, 61(13), 3167-3178.
27. Berto F, Lazzarin P. Recent developments in brittle and quasi-brittle failure assessment of engineering materials by means of local approaches. Materials Science & Engineering, 2014, 75, 1-48.
28. Abadias G, Chason E, Keckes J, Sebastiani M, Thompson GB, Barthel E, Doll GL, Murray CE, Stoessel CH, Martinu L. Stress in thin films and coatings: Current status, challenges, and prospects, Journal of Vacuum Science & Technology A: Vacuum, Surfaces and Films, 2018, 36(2):020801.

29. Van Leeuwen M, Kamminga JD, Mittemeijer EJ. Diffraction stress analysis of thin films: Modeling and experimental evaluation of elastic constants and grain interaction, Journal Of Applied Physics, 1999, 86, 1904-1914
30. Holden TM, Root JH, Holt RA, Hayashi Neutron-diffraction measurements of stress, Physica B: Condensed Matter, 1995, 213&214, 793-796
31. Bemporada E, Brisottob M, Deperob LE, Gelfib M, Korsunskyc AM, Luntc AJG, Sebastiania A critical comparison between XRD and FIB residual stress measurement techniques in thin films, Thin Solid Films, 2014, 572, 224-231
32. Grabner L. Spectroscopic technique for the measurement of residual stress in sintered Al_2O_3, Journal Applied Physics, 1978, 49, 580-583
33. Parnas L, Bilir ÖG, Tezcan E. Strain gage methods for measurements of opening mode stress intensity factor. Engineering Fracture Mechanics, 1996, 55(3), 485-492.
34. Zike S, Mikkelsen LP. Correction of Gauge Factor for Strain Gauges Used in Polymer Composite Testing. Experimental Mechanics, 2013,54(3), 393-403.
35. Poornachandra Pandit, Ansal VK, Venkataramana, Parthiban P, Experimental investigation on corroded reinforced concrete beam in coastal environment using strain gauges, International Journal of Engineering and Innovative Technology, 2013,3(5), 416-422.
36. Freddi A., Olmi G., Cristofolini L. Introduction to the Application of Strain Gages. In: Experimental Stress Analysis for Materials and Structures. Springer Series in Solid and Structural Mechanics, 2015.
37. Liu GZ, Liu H, Wei AQ, Xiao, JL1, Wang P, Li SZ. A new device for stress monitoring in continuously welded rails using bi-directional strain method. Journal of Modern Transportation, 2018,26(3), 179-188.
38. Hu XY, Wang BW, Ji H. A Wireless Sensor Network-Based Structural Health Monitoring System for Highway Bridges. Computer-Aided Civil and Infrastructure Engineering, 2013,28(3), 193-209.
39. Tegtmeier FL. Strain gauge based microsensor for stress analysis in building structures. Measurement, 2008,41(10), 1144-1151.
40. Teomete E, Kocyigit OI. Tensile strain sensitivity of steel fiber reinforced cement matrix composites tested by split tensile test. Construction and Building Materials, 2013,47, 962-968.
41. Gomes PTV, Maia NS, Mansur TR, Palma ES. Temperature effect on strain measurement by using weldable electrical resistance strain gages. Journal of Testing and Evaluation, 2003,31(5), 363-369.
42. Afonin GV, Mitrofanov YP, Kobelev NP, Pinto MWD, Wilde G, Khonik VA. Relationship between the enthalpies of structural relaxation, crystallization and melting in metallic glass-forming systems. Scripta Materialia, 2019,16*6*, 6-9.

Figures

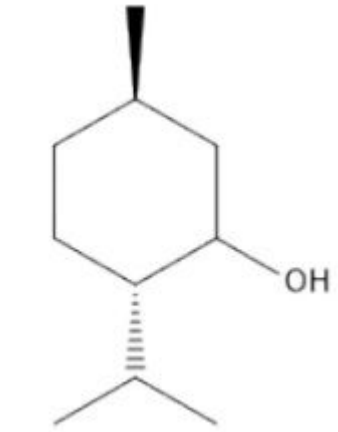

Figure 1

Molecular structure of L-menthol

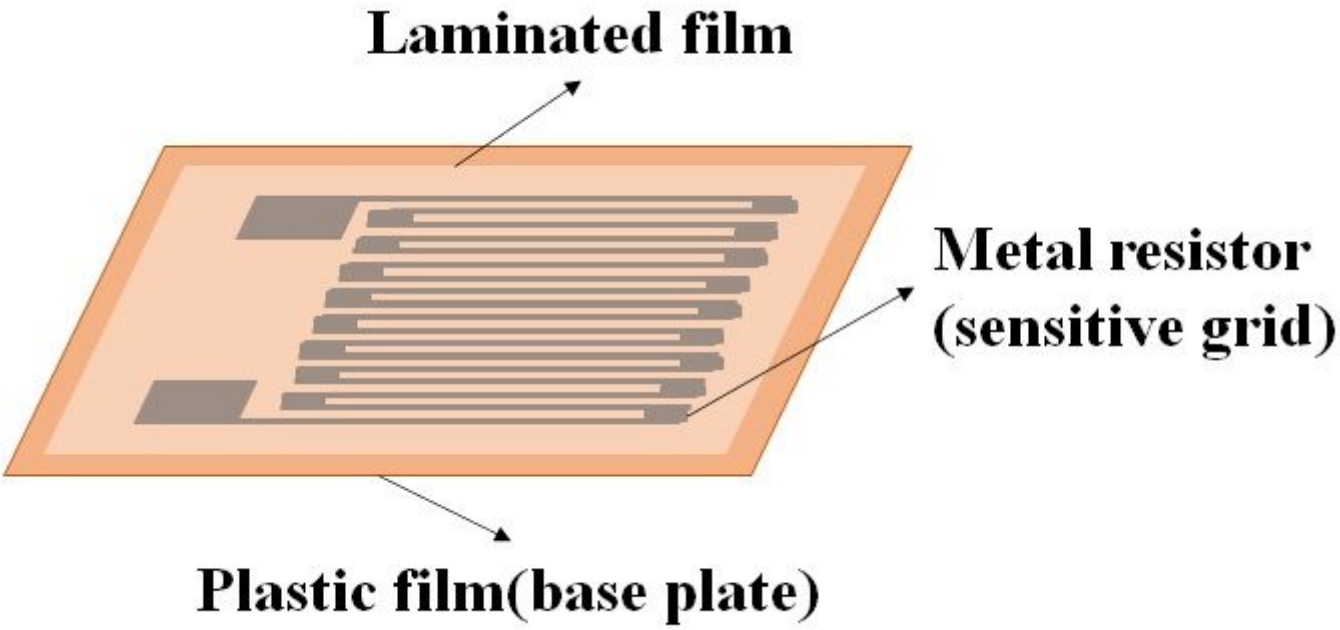

Figure 2

The schematic of a strain gauge

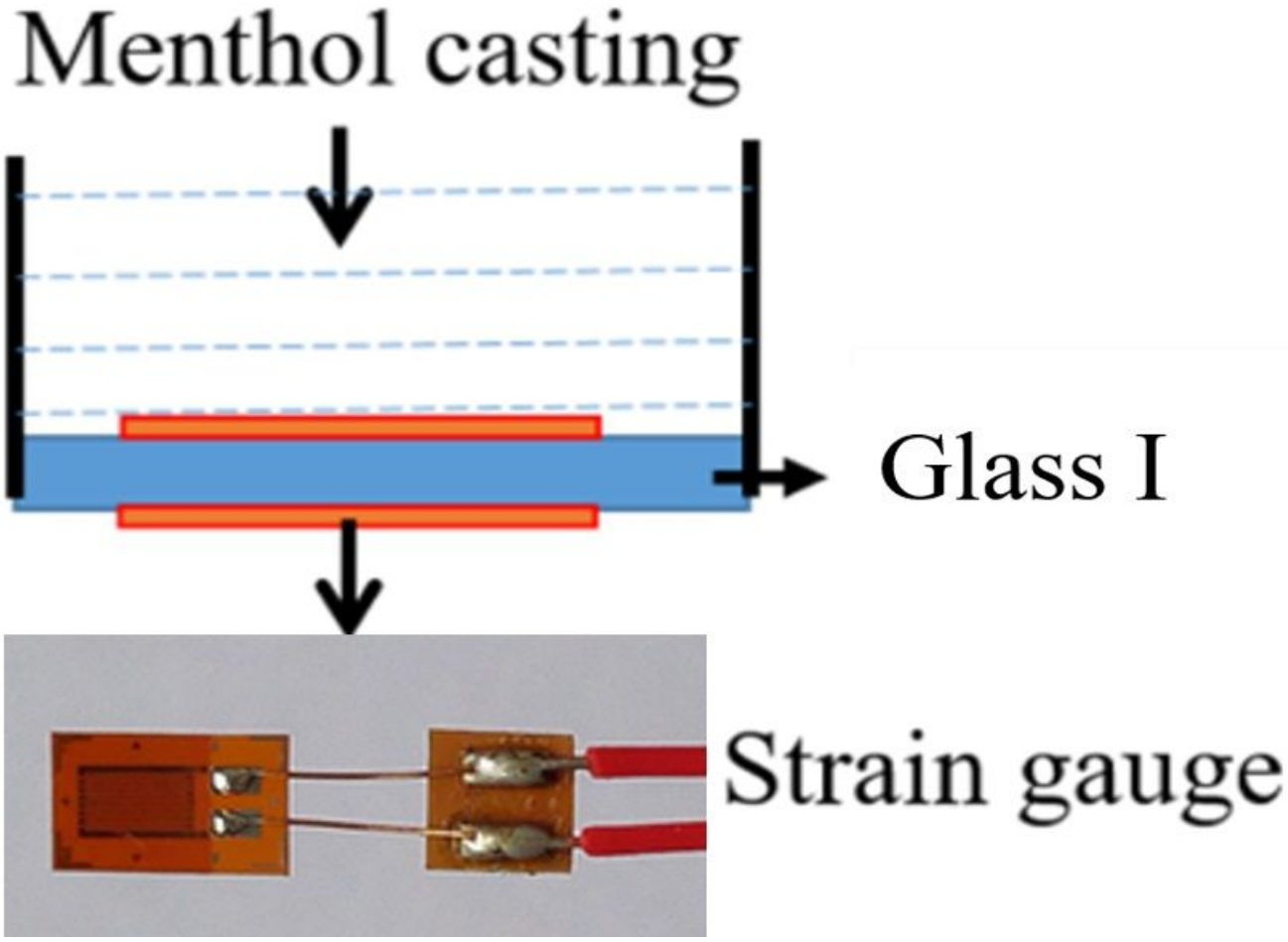

Figure 3

Schematic of strain tests on glass I sample

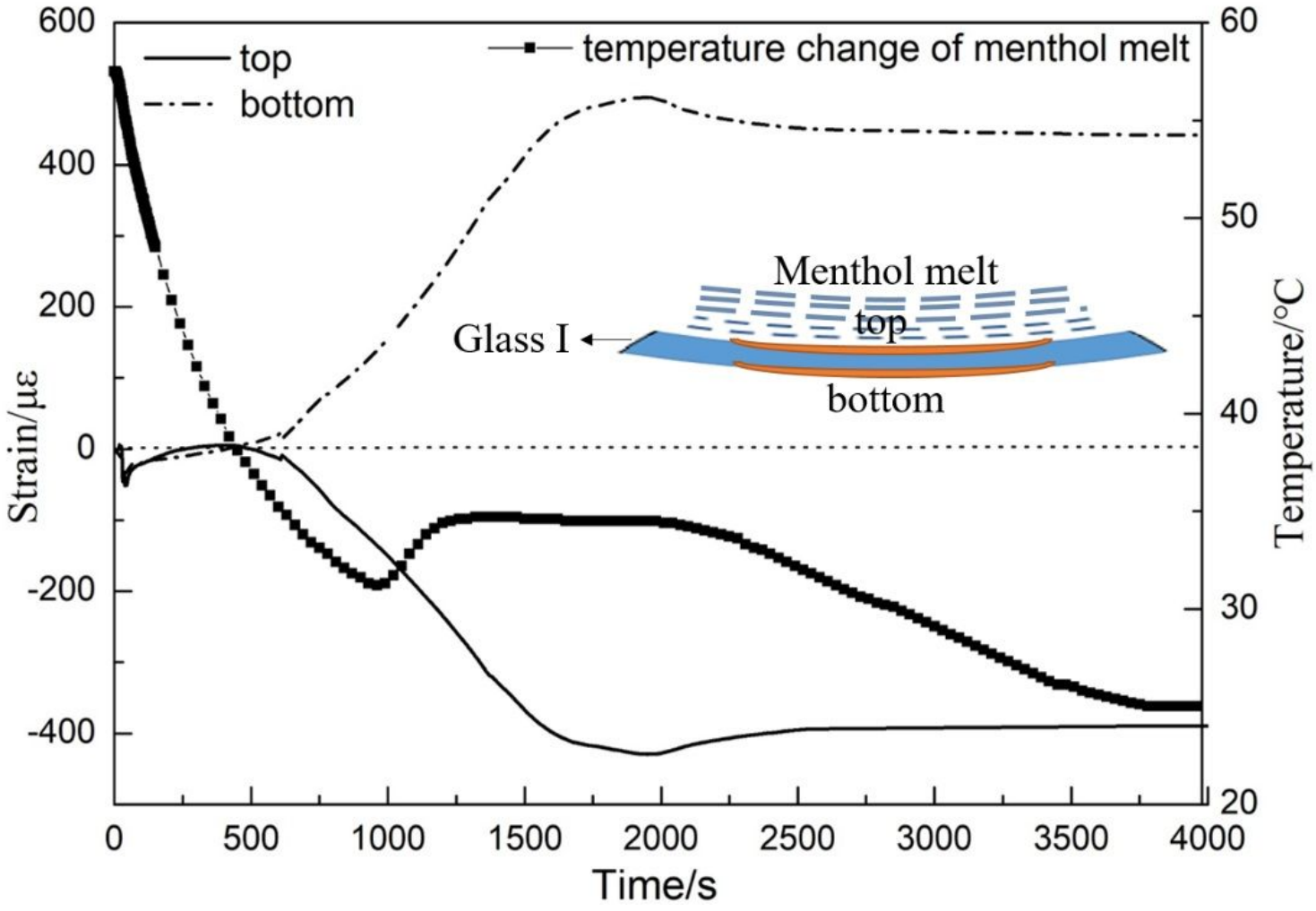

Figure 4

Results of strain tests on glass I sample (2mL 60°C melt applied on an area of 18mm×18mm; thickness is around 10mm)

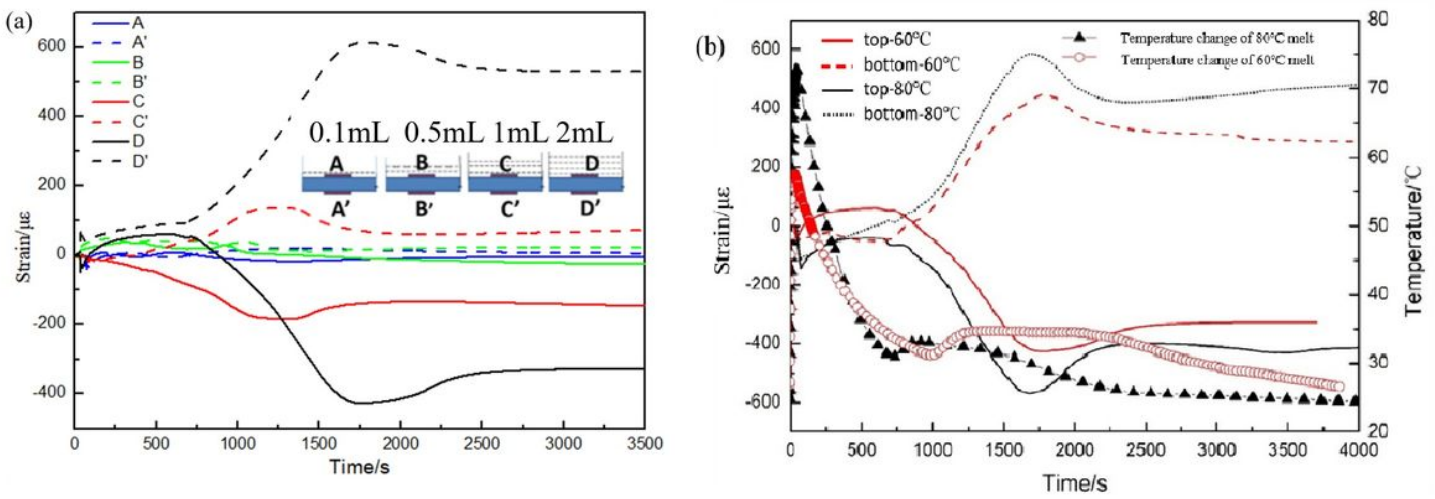

Figure 5

Results of strain tests on glass I samples with a) different amounts of menthol melts, applied on areas of 18mm×18mm; thicknesses are around 1mm, 3mm, 5mm, 10mm respectively; b) 2mL menthol melts of 60 or 80 ℃, applied on areas of 18mm×18mm; thicknesses are around 10mm.

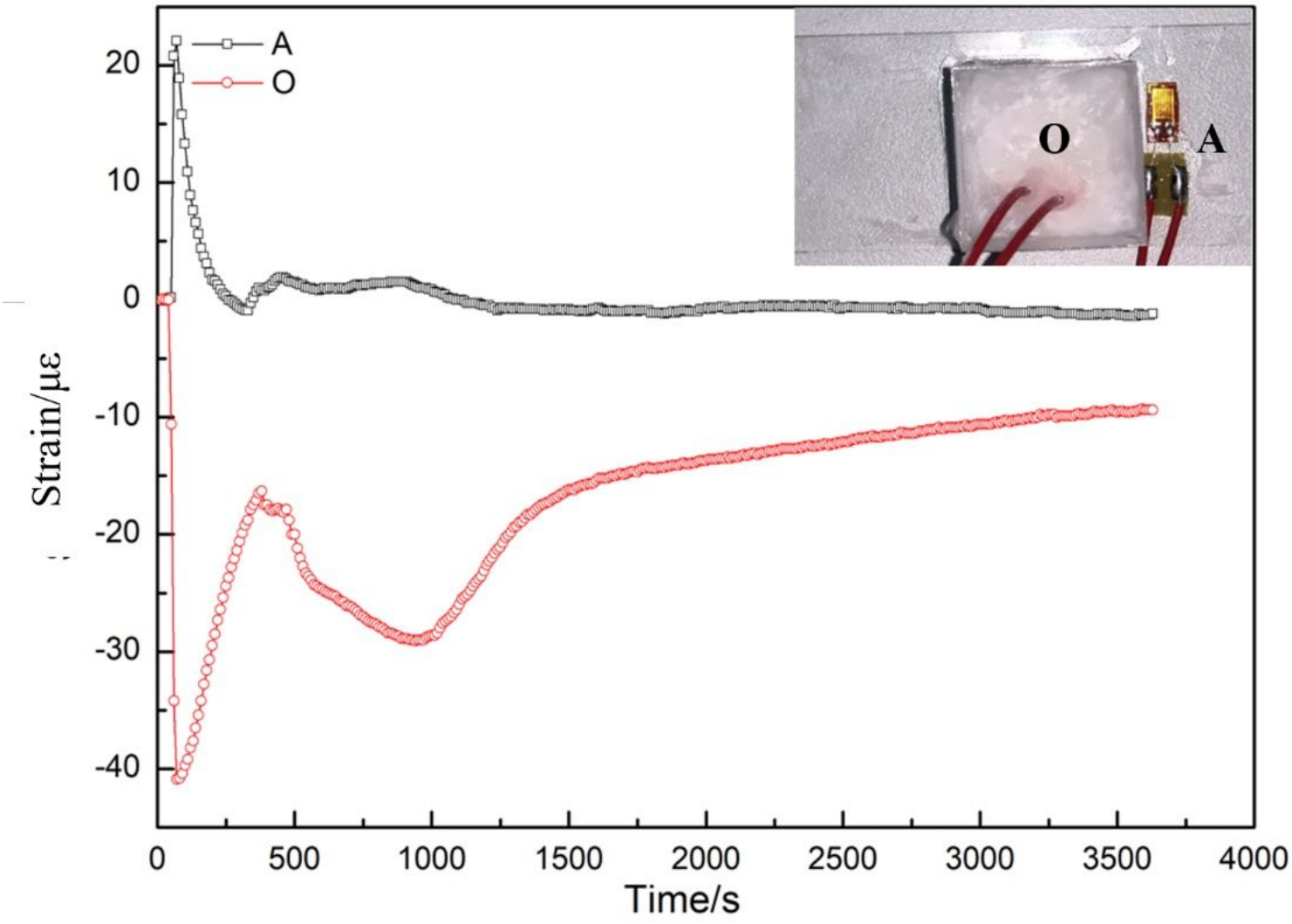

Figure 6

Results of strain tests on Glass II sample (2mL 60℃ menthol melt applied on an area of 18mm×18mm; thickness is around 10mm)

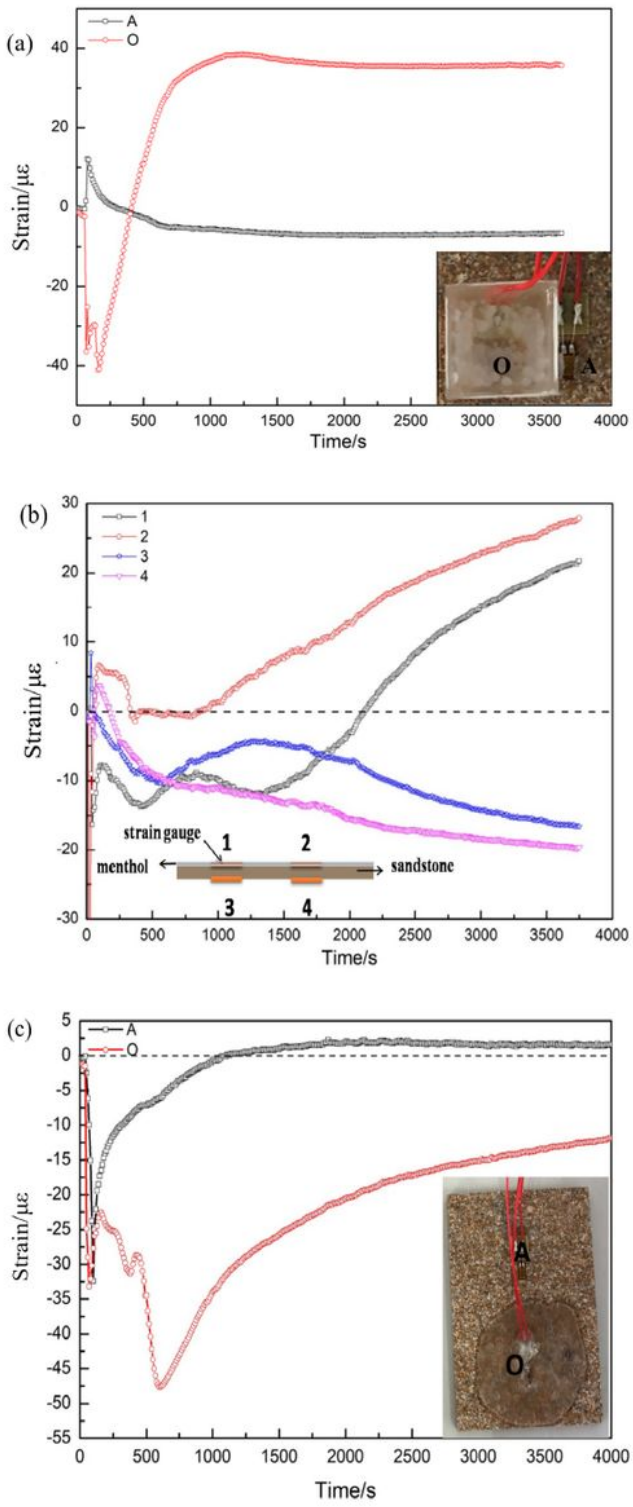

Figure 7

The strain produced by the solidification of menthol melt (60 ℃) on the Yungang sandstones. a) 2 strain gauges setup (2mL melt applied on an area of 18mm×18mm, thickness is around 10mm); b) 4 strain gauges setup (2mL melt applied on an area of 25mm×75mm, thickness is around 2mm); c) 2 strain gauges setup (1mL melt applied on a larger sandstone sample, applying area is about 60 mm in diameter and 1mm in thickness)

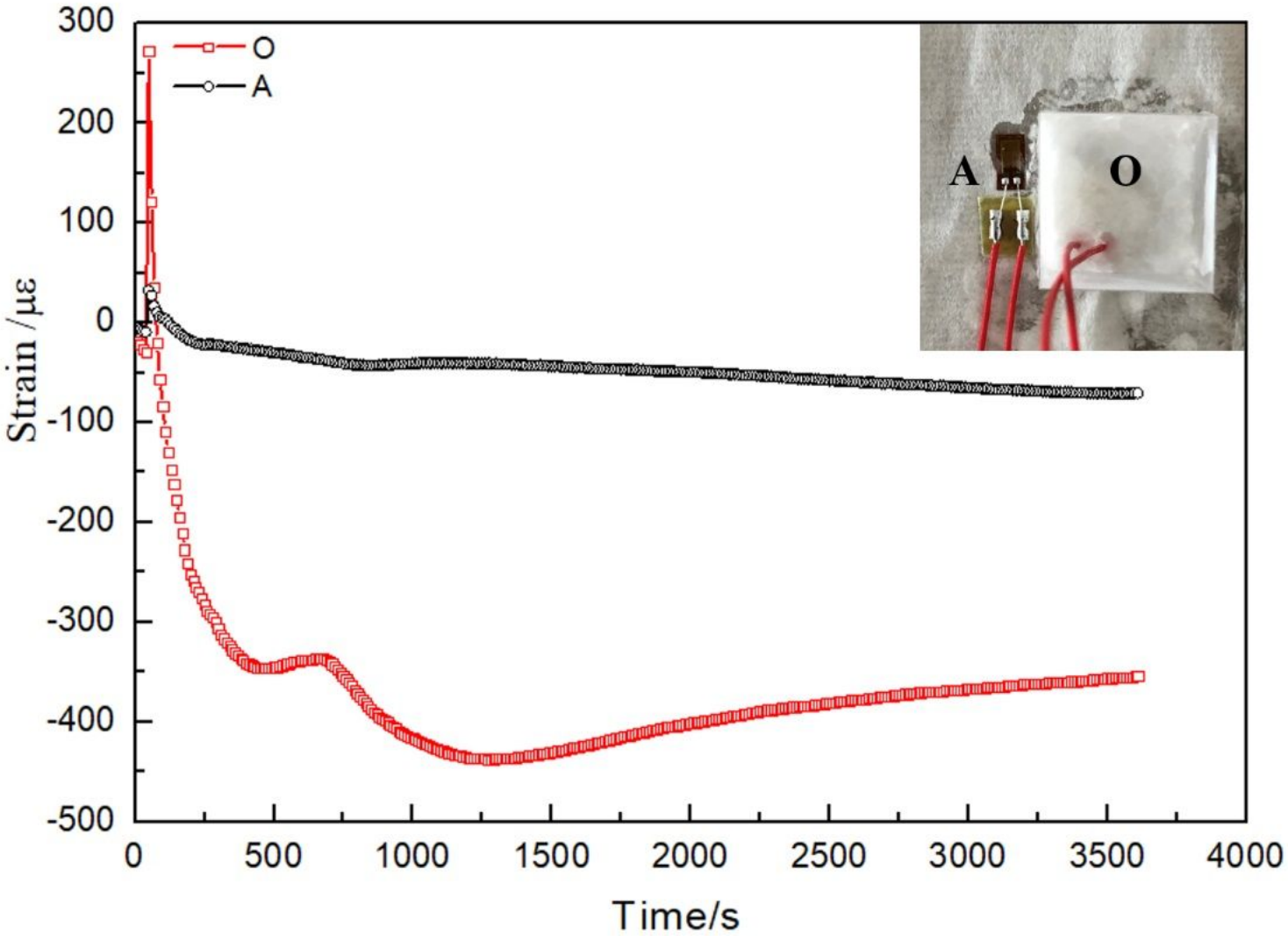

Figure 8

Results of strain tests on a rice paper (2mL 60℃ menthol melt applied on an area of 18mm×18mm; thickness is around 10mm)

Supplementary Files

This is a list of supplementary files associated with this preprint. Click to download.

- stresspaperHS0526SI.pdf